Precipitation-driven gamma radiation enhancement over the Atlantic Ocean

Susana Barbosa[1], Nuno Dias[1], Carlos Almeida[1], Guilherme Silva[1], António Ferreira[1], António Camilo[2], Eduardo Silva[1]

[1]INESC TEC - INESC Technology & Science, Porto, Portugal
[2]CINAV, Marinha, Lisboa, Portugal

Key Points:

- Precipitation-driven enhancements in gamma radiation are detected in the oceanic environment.
- Gamma radiation enhancements are found in the open ocean at large distances (+ 500 km) from the nearest coastline.
- The enhancements result from precipitation scavenging of radioactive elements attached to aerosols, likely both radon progeny and beryllium-7 radionuclides.

Corresponding author: Susana Barbosa, `susana.a.barbosa@inesctec.pt`

Abstract

Gamma radiation over the Atlantic Ocean was measured continuously from January to May 2020 by a NaI(Tl) detector installed on board the Portuguese navy's ship NRP Sagres. Enhancements in the gamma radiation values are identified automatically by an algorithm for detection of anomalies in mean and variance as well as by visual inspection. The anomalies are typically +50% above the background level and relatively rare events ($\sim < 10\%$ of the days). All the detected anomalies are associated with simultaneous precipitation events, consistent with the wet deposition of scavenged radionuclides. The enhancements are detected in the open ocean at large distances (+ 500 km) from the nearest coastline suggesting the contribution from radionuclides other than radon progeny - which has a predominantly terrestrial source - likely beryllium (Be-7), originated in the earth's atmosphere by cosmic radiation. Both radon progeny and Be-7 radionuclides attach readily to aerosols after formation, and low abundance of aerosols is suggested to explain the cases of precipitation and absence of gamma radiation enhancements. These results have implications for the use of radionuclides as tracers of transport and residence time of aerosols in the marine boundary layer.

1 Introduction

Gamma radiation is well known to exhibit significant enhancements associated with precipitation events (e.g. Fujinami (1996); Yakovleva et al. (2016); Bossew et al. (2017); Melintescu et al. (2018)). The increase in gamma radiation results mainly from the wet deposition of Rn-222 progeny, mainly Pb-214 and Bi-214 (e.g. Livesay et al. (2014); Bottardi et al. (2020); Zelinskiy et al. (2021)). The concentration of radon progeny in precipitation is not correlated with the concentration of radon progeny in air (Fujinami, 1996), suggesting that the scavenging of radionuclides to the ground is dominated by processes within the clouds - nucleation scavenging and interstitial aerosol collection by cloud or rain droplets - rather than by processes below the cloud base (e.g. Takeuchi and Katase (1982); Paatero and Hatakka (1999)). The increase in gamma radiation associated with precipitation depends on the history of the corresponding contributing air mass (Paatero, 2000; Inomata et al., 2007; Mercier et al., 2009; Barbosa et al., 2017) but no clear association has been found between precipitation (intensity, amount and duration), and the resulting enhancement in gamma radiation (Fujinami, 1996; Burnett et al., 2010; Cortes et al., 2001; Greenfield et al., 2003; Datar et al., 2020). The connection between the temporal variability of gamma radiation and precipitation is not straightforward as a result of the complex interplay of factors such as the amount and intensity of precipitation, the cloud's thickness and base height, and the atmospheric concentration of sub-micron aerosols, all influencing the scavenging of radon progeny (Barbosa et al., 2017).

Although gamma radiation peaks driven by precipitation have been studied in numerous and varied settings, here we report, for the first time, gamma enhancements associated with precipitation in the oceanic environment. In the framework of project SAIL (Space-Atmosphere-Ocean Interactions in the marine boundary Layer) gamma radiation has been measured continuously on board the Portuguese navy ship NRP Sagres (Barbosa, Dias, et al., 2022). Over the ocean radon exhalation from the surface is negligible, and the substantial contribution over land of terrestrial environmental radioactivity does not exist. Thus gamma radiation in a marine setting mainly reflects atmospheric rather than surface effects. Gamma radiation is then determined by cosmic rays and its interaction with gas molecules in the atmosphere, and by radionuclides attached to atmospheric aerosols. In the present study we document enhancements in gamma radiation over the Atlantic ocean from high-resolution gamma radiation measurements. The data are described in section 2, the analysis is detailed in section 3 and concluding remarks are provided in section 4.

2 Data

Data considered in this study consist in gamma radiation (section 2.1) and meteorological measurements (section 2.2) performed over the Atlantic ocean from January to May 2020 on board the sail ship NRP Sagres. Figure 1 shows the map of the ship's trajectory since its departure from Lisboa in January 5th 2020. The trip was initially planned to last for 371 days, but was interrupted due to the COVID-19 pandemic and subsequent restrictions in port activities. On March 25th the ship arrived to Cape Town for refueling and supplies, departing the same day back to Portugal, instead of resuming the trip into the Indian Ocean as originally planned. The ship arrived to Lisboa on May 10th, after a stop for repairs at the port of Praia, Cape Verde. Overall data completion is > 95%, with two short periods of data loss due to issues in the onboard computer and storage systems, which occurred on March 8th and 9th (during the trip from Buenos Aires to Cape Town) and then from 4 to 6 April, in the leg from Cape Town to Lisboa.
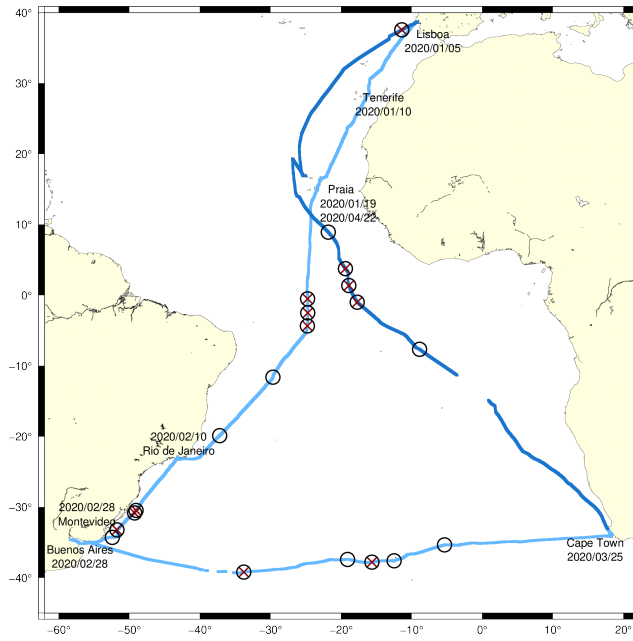

Figure 1. Map of the trajectory of NRP Sagres ship. The data points represented by light blue correspond to the Lisboa - South Africa leg of the trip, and darker blue represents the return trip from South Africa to Lisboa. The symbols ◯ mark the location of the rain events listed in Table 1 and symbols × represent the location of the gamma anomalies listed in table 2. Blanks denote points with no available data due to computer issues (<   5% of the total data collected).

2.1 Gamma radiation data

Gamma measurements are performed with a 3" NaI(Tl) scintillator (Scionix, the Netherlands) equipped with an electronic total count single channel analyzer for acquiring total counts of gamma radiation in the 475 keV to 3 MeV energy range. The selection of this energy range enables the reduction of Compton background in the 50–475 keV low-energy range, improving the sensitivity of radon progeny measurements (Zafrir et al., 2011). The NaI(Tl) scintillator is encased in a water-proof container designed for underwater measurements, in order to protect the instrument from harsh marine con-

86 ditions. The sensor is installed on the mizzen mast of the ship, at a height of ~ 20 m.
87 Counts are acquired at a sampling rate of 1-second and further aggregated into counts
88 per minute. Further details on data management and pre-processing are described in the
89 SAIL project's data management plan (Barbosa & Karimova, 2021).
90   The 1 minute time series of gamma radiation counts is presented in Figure 2. Ex-
91 cept for the evident ocean-land contrast, the temporal variation of gamma radiation counts
92 is small, being more prominent in the first month of the series and very stable afterwards.
93 The long-term component of gamma radiation variability is estimated by robust local
94 regression (Cleveland et al., 1992) and represented by the colored solid line in Figure 2.
95 The measurements performed over land during the stops of the ship along its journey,
96 represented in gray in Figure 2 (top), are not further considered, as this work focus only
97 on the observations of gamma radiation over the ocean. Thus the gamma radiation time
98 series considered hereafter, displayed in Figure 2 (bottom), consists in the 1-minute gamma
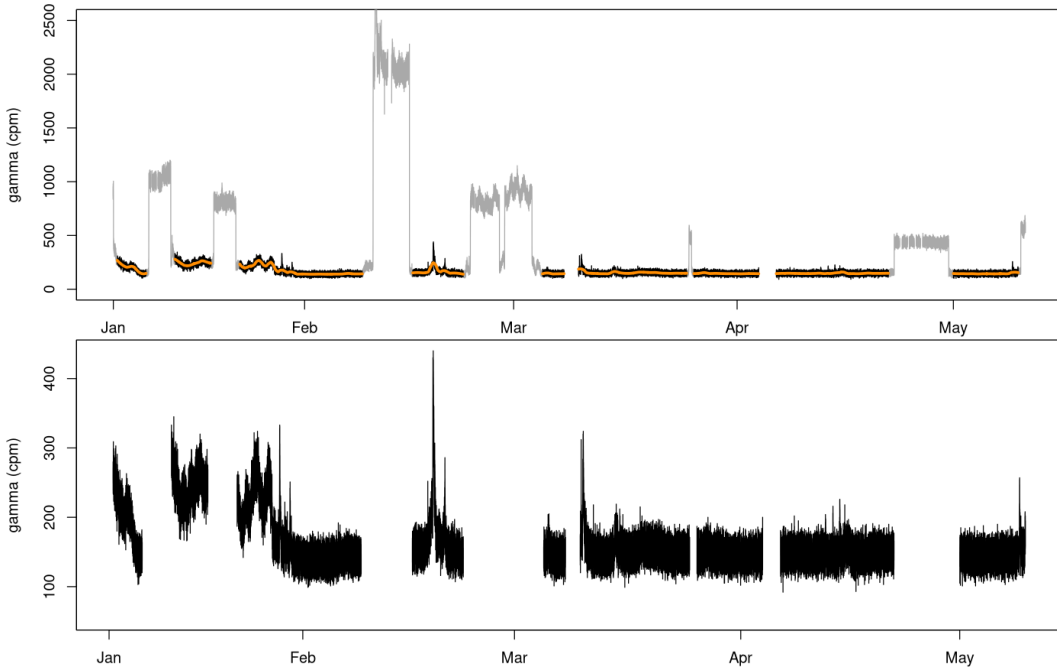99 radiation counts measured exclusively in the marine environment (126 days in total).

Figure 2. Time series of gamma radiation data. Top: complete 1-minute series with land measurements represented in gray and long-term variability by the solid colored line. Bottom: time series of marine-only 1-minute gamma radiation counts.

100 ## 2.2 Meteorological data

101   Two distinct types of meteorological data are available from the SAIL campaign:
102 automatic data collected by sensors, with no need of human intervention, and data col-
103 lected by human observers. The meteorological optical range is measured very 1-minute
104 by a visibility sensor SWS050 (Biral, UK) located at the same height and on the same
105 mast as the gamma radiation instrument. Rain, and basic meteorological parameters such
106 as atmospheric pressure, temperature and wind, are collected in a non-automatic way
107 by the ship's crew every 1-hour as part of the navy's operational routine during navi-
108 gation (no meteorological information is available when the ship is docked). Rainfall events
109 are recorded in a qualitative way (e.g. light, moderate, drizzle). The geographic loca-
110 tion of rain events is shown as ◯ in Figure 1. Table 1 summarizes the available infor-

Table 1. Rain events recorded by navy's observers during the NRP Sagres trip.

date	time (UTC)	rain
2020-01-28	01:00	drizzle
2020-01-28	20:00	moderate
2020-01-28	22:00	drizzle
2020-01-29	11:00-13:00	drizzle
2020-01-30	05:00-06:00	drizzle
2020-02-03	07:00	drizzle
2020-02-06	17:00	drizzle
2020-02-18	21:00	drizzle
2020-02-22	17:00	drizzle
2020-03-10	03:00-04:00	light
2020-03-10	08:00	moderate
2020-03-10	9:00-14:00	light
2020-03-14	07:00	light
2020-03-14	08:00-09:00	moderate
2020-03-14	15:00	light
2020-03-16	01:00	light
2020-03-16	07:00	light
2020-03-18	05:00	drizzle
2020-04-08	09:00	light
2020-04-12	14:00	moderate
2020-04-14	06:00	drizzle
2020-04-14	12:00	drizzle
2020-04-16	21:00	drizzle
2020-05-09	05:00	drizzle

mation in terms of rain occurrences during the whole trip. In general rain was not a frequent event, as it is registered in only 16 days out of a total of 126. Times were originally recorded as local time but are presented as coordinated universal time (UTC), as for all the other data. Rain registered at a given hour corresponds to rain observed within the previous hour.

3 Analysis

3.1 Detection of gamma radiation anomalies

For the detection of anomalies in the marine gamma radiation time series (Fig. 2, bottom), two complementary distinct approaches are used: an automatic method and visual inspection of the time series. The automatic detection of anomalies is performed using the Collective And Point Anomaly (CAPA) algorithm (Fisch et al., 2018). The outcomes of the algorithm are very much dependent on the pre-processing of the time series in terms its standardization and handling of missing values. This is particular critical in this case due to the numerous gaps in the time series. Thus for the application of the CAPA procedure the following pre-processing steps are taken: i) the long-term variability signal (represented by the solid line in Fig. 2 top) is subtracted from the series for stabilization of the mean; and ii) the gaps are filled by replacing the missing values by values resulting from a normal distribution with the same mean and variance as the gamma radiation time series. The CAPA algorithm is then applied to the pre-processed time series using a penalty for control of false positives of $2 \times \frac{1+\phi}{1-\phi} log(n)$, where ϕ is set as 0.9 and n is the length of the time series. The results are displayed in Figure 3. In
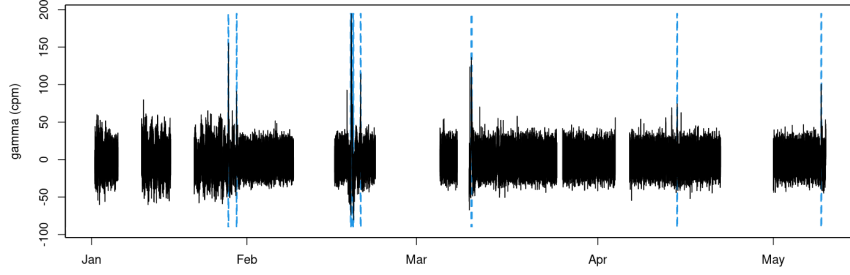
Figure 3. Detrended time series of gamma radiation. The anomalies identified by the CAPA algorithm are represented by the vertical dashed lines.

Table 2. Anomalies identified in the marine gamma radiation observations by visual inspection and by using the CAPA algorithm. It is also indicated whether these periods identified as anomalous correspond to rain events or anomalies in visibility.

date	time (UTC)	Visual detection	CAPA algorithm	Rain	Visibility
2020-01-28	19:00-21:00	✓	✓	✓	✓
2020-01-29	13:00-14:00	✓	-	✓	✓
2020-01-30	05:00-07:00	✓	✓	✓	✓
2020-02-18	19:00-24:00	✓	✓	✓	✓
2020-02-19	01:00-02:00	✓	✓	-	✓
2020-02-20	10:00-12:00	✓	✓	-	✓
2020-03-10	08:00-16:00	✓	✓	✓	✓
2020-03-15	10:00-11:00	✓	-	-	✓
2020-04-12	14:00-16:00	✓	-	✓	✓
2020-04-13	14:30-15:30	✓	-	-	✓
2020-04-14	13:00-14:00	✓	✓	✓	✓
2020-05-09	04:00-06:00	✓	✓	✓	✓

a conservative approach (mainly determined by the penalty value for control of false positives), a total of 8 anomalies are detected. Visual inspection confirms these, and further identifies 4 additional candidate anomalies in gamma radiation, summarized in Table 2. The geographic location of these 12 anomalies is displayed in Figure 1.
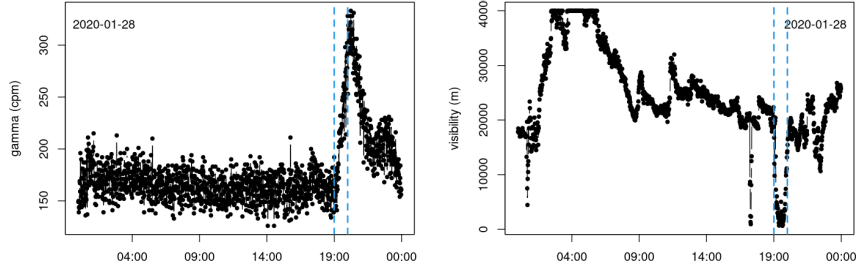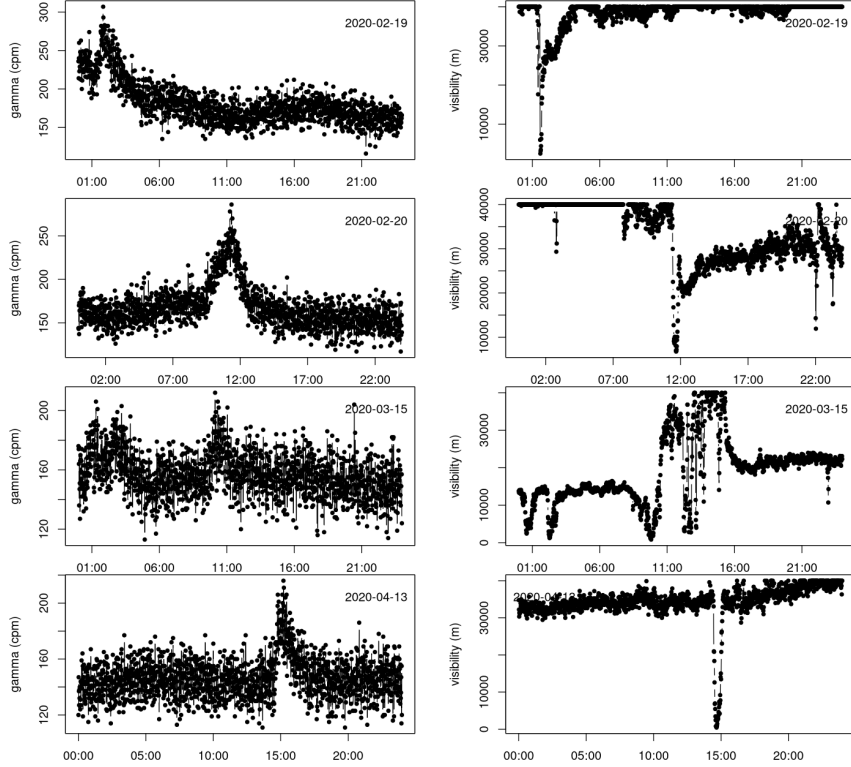
3.2 Characteristics of marine gamma anomalies

Table 3 summarizes the occurrence of anomalies in the gamma radiation time series as a function of the rainfall information. From a total of 126 days with gamma radiation measurements over the ocean, gamma anomalies are identified in only 12 days ($< 10\%$). Most of these anomalies ($\sim 65\%$) are associated with the occurrence of rain according to the available meteorological information from human observers. They are also associated with concurrent anomalies in the meteorological optical range from the visibility sensor, as illustrated in Figure 4. Only 4 gamma radiation anomalies occur in days for which rain was not registered by human observers. And in all these 4 cases the anomalies in gamma radiation are associated with simultaneous sharp drops in visibility, as shown in Figure 5. Thus it seems likely that also these gamma radiation anomalies are driven by precipitation which apparently failed to be registered by the human observers.

Although all enhancements in gamma radiation are associated with the occurrence of precipitation, the reverse is not true, i.e. the occurrence of precipitation is not nec-

Table 3. Contingency table for the number of occurrences (in days) of rain and gamma radiation anomalies.

	number of days rain	number of days no rain	
gamma anomaly	8	4	12
no gamma anomaly	8	106	114
	16	110	126

Figure 4. Detail (28th January 2020) of 1-minute time series of gamma radiation counts (left) and visibility (right). The vertical dashed lines represent the period of occurrence of moderate rain as indicated in the available meteorological information.

Figure 5. Detail of 1-minute time series of gamma radiation counts (left) and visibility (right) for the days in which an anomaly is identified in gamma radiation but rain is not registered in the navy's meteorological observations.
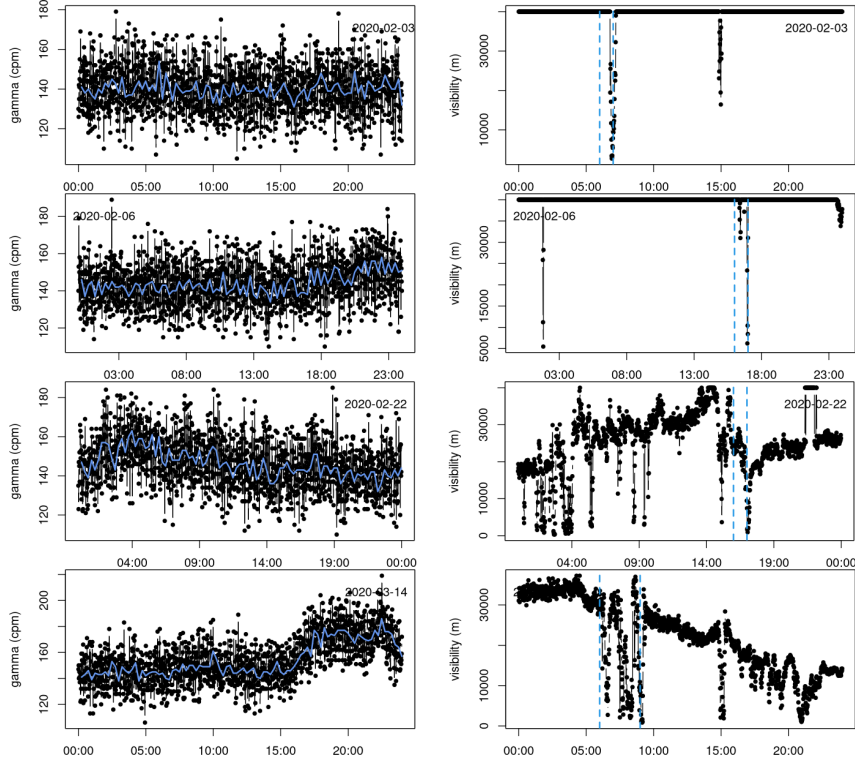
Figure 6. Detail of 1-minute time series of gamma radiation counts (left) and visibility (right) for the days with occurrence of precipitation but no gamma anomalies. The solid (blue) line represents the 15-minute running median of gamma radiation counts. The vertical dashed lines represent the period of occurrence of rain from the available meteorological information.

essarily associated with an anomaly in gamma radiation. For a total of 16 days with registered rain events, half do not have a corresponding anomaly in the gamma radiation counts. These cases are detailed in Figures 6 and 7. Comparison of the visibility measurements with the meteorological information in Table 1 shows strong consistency between human-recorded and instrumental information. Only in one case (16th April 2020 - Figure 7) the visibility data does not point to the occurrence of rain, in disagreement with the qualitative information of early morning drizzle. In all the remaining cases visibility measurements are very consistent with the qualitative rain data information available. Thus the absence of gamma anomalies (or in two cases - 2020-03/18 and 2020-04-08 - only very small increases barely detectable within the noise level) is not related to eventual errors in the qualitative rain information.

Table 4 shows the % enhancement in gamma radiation and the corresponding distance to the nearest coastline for all days with an anomaly in gamma radiation and/or occurrence of rain. The % enhancement is obtained for each day in which a gamma anomaly was identified by computing the difference of the maximum gamma value relative to the average background value of that day. The distance to the nearest coastline is computed using the Generic Mapping Tools (GMT) software (Wessel et al., 2019) using its low resolution coastline (Wessel & Smith, 1996). Figure 8 displays the % increase in gamma radiation as a function of the distance to the nearest coastline and rain characteristics. Inspection of Table 4, Figure 8, (and also of the map in Figure 1) doesn't reveal any clear association between gamma radiation anomalies and the type of precipitation as qual-
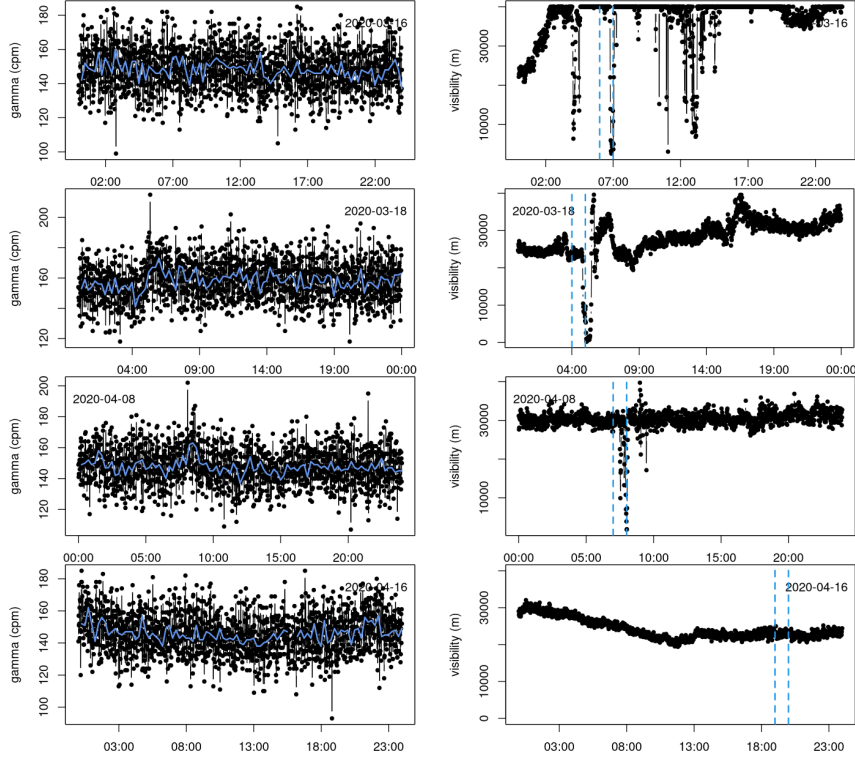
Figure 7. same as in Figure 6.

itatively recorded by human observers. It is also not observed any consistent association between the enhancement in gamma radiation and the distance to the nearest landmass.

4 Discussion and conclusions

This work documents, for the first time, enhancements of gamma radiation over the ocean associated with the occurrence of precipitation. Most of these enhancements were observed in the southern hemisphere and at varying distances from land, from about 100 km to more than 1500 km to the nearest shoreline.

As it is also the case for gamma radiation enhancements over land, a clear association between the enhancement in gamma radiation and the amount and intensity of precipitation is not discernible, although here the analysis is limited by the low temporal resolution (1 hour) and the qualitative nature of precipitation observations. Still the information from human observation is in very good agreement with the meteorological optical range measured by the visibility sensor, giving confidence to the use of both types of data.

All the anomalies identified in the marine gamma radiation time series are associated with concurrent occurrence of rain (either explicitly registered by human observation or inferred by visibility data). This fact is consistent with the wet deposition mechanism being the main driver of enhancements in gamma radiation at the earth's surface. However, the enhancements in gamma radiation are observed very far from land, in the middle of the Atlantic ocean, and doesn't seem to be determined by the distance to the nearest coastline, which would be expected in case of radionuclides with a predominantly terrestrial source, such as radon and its progeny. Radon originates exclusively from the earth's surface, and the oceanic source is very small (Chambers et al., 2016), the total

Table 4. Approximate distance to the nearest coastline for all the days with an anomaly in gamma radiation and/or occurrence of rain. (1) denotes days in which rain is inferred from visibility measurements and (2) rain occurrence suspect (not confirmed by visibility data).

date	rain	increase in gamma (%)	distance to land (km)
2020-01-28	moderate	99	927
2020-01-29	drizzle	33	866
2020-01-30	drizzle	70	849
2020-02-03	drizzle	-	677
2020-02-06	drizzle	-	272
2020-02-18	drizzle	142	118
2020-02-19	(1)	78	112
2020-02-20	(1)	79	81
2020-02-22	drizzle	-	105
2020-03-10	moderate	95	1666
2020-03-14	light/moderate	-	564
2020-03-15	(1)	36	263
2020-03-16	light	-	35
2020-03-18	drizzle	-	649
2020-04-08	light	-	600
2020-04-12	moderate	40	847
2020-04-13	(1)	49	948
2020-04-14	drizzle	54	820
2020-04-16	(2)	-	639
2020-05-09	drizzle	73	213

oceanic contribution to radon in the global atmosphere being estimated to be only about 2% of all the radon exhaled from continents (Wilkening & Clements, 1975).

A further potential contribution to the observed enhancement in gamma radiation is Beryllium-7 (Be-7), a radionuclide produced in the earth's upper atmosphere by cosmic radiation through the spallation of nitrogen and oxygen. It has an half-life of ~ 53 days, emitting gamma radiation with energy of $\sim$ 477.6 keV. After its formation Be-7 readily becomes associated with aerosols in the sub-micron size range (e.g (Ioannidou et al., 2005)) and is then subject to complex horizontal and vertical atmospheric transport processes (Kaste et al., 2002). Precipitation scavenging is the dominant ($\sim 90\%$) process of removal of Be-7 from the atmosphere (Kaste et al., 2002; Kusmierczyk-Michulec et al., 2015) and low precipitation rates during drizzles are particularly efficient in scavenging Be-7 by fine droplets (Ioannidou & Papastefanou, 2006).

The enhancements in total gamma radiation documented in the present study can't be unequivocally attributed to a specific radionuclide, as the measurements are of total gamma radiation in an energy range (0.475-3 MeV), optimal for radon progeny measurements but that also includes gamma radiation emitted by Be-7. It is thus likely that the data includes the contribution of both radionuclides, with enhancements observed very far from land, at locations where radon gas concentration is expected to be minimal, reflecting mainly the cosmic-radiation generated Be-7 radionuclide.

The cases in which precipitation does not produce an increase in gamma radiation possibly reflect situations of low abundance of aerosols in the marine boundary layer, as both radon progeny and beryllium-7 radionuclides attach rapidly to aerosols after formation. No systematic relationship is observed between the enhancement in gamma radiation and the rain type nor the distance to land.
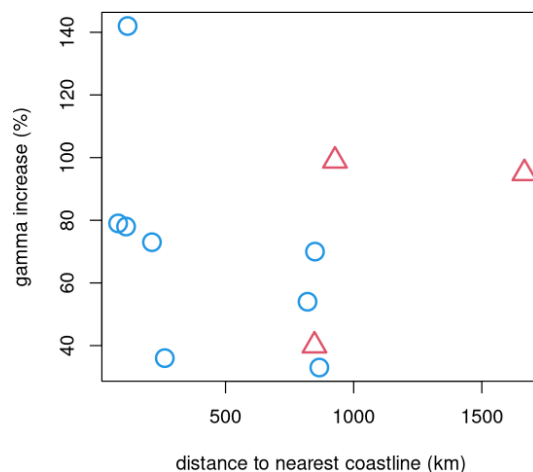
Figure 8. Enhancement in gamma radiation (percentage relative to the daily average background level) as a function of the distance to the nearest coastline. Symbols △ represent anomalies associated with rain events classified as moderate and symbols ◯ rain classified as drizzle (the cases for which there is no meteorological information and rain is inferred from visibility data are considered as drizzle).

Further investigation and additional (energy-discriminating) measurements are needed to confirm these results and increase understanding on planetary environmental radioactivity and the use of radionuclides as tracers of cloud scavenging and precipitation processes, with implications for the use of radionuclides as tracers of transport and residence time of aerosols in the marine boundary layer.

5 Open Research

Raw measurements from the SAIL campaign are available upon request (Barbosa et al., 2021). The datasets of processed measurements used in this manuscript are publicly available: gamma radiation data (Barbosa, Almeida, et al., 2022a) and visibility data (Barbosa, Almeida, et al., 2022b). The analysis was performed using the R software (R Core Team, 2022). Maps were created with the Generic Mapping Tools (GMT) software (Wessel et al., 2019).

References

Barbosa, S., Almeida, C., Amaral, G., Dias, N., Ferreira, A., Camilo, A., & Silva, E. (2022a). Sail - gamma radiation data [dataset]. doi: 10.6084/m9.figshare.20393931.v1

Barbosa, S., Almeida, C., Amaral, G., Dias, N., Ferreira, A., Camilo, A., & Silva, E. (2022b). *Sail - visibility data [dataset].* doi: 10.6084/m9.figshare.19692394.v2

Barbosa, S., Almeida, C., Guilherme, A., Dias, N., Ferreira, A., et al. (2021). *Raw data collected onboard the sagres ship during the sail project campaign [dataset].* INESC TEC research data repository. doi: https://doi.org/10.25747/

b2ff-kg31

Barbosa, S., Dias, N., Almeida, C., Amaral, G., Ferreira, A., Lima, L., ... Silva, E. (2022). An holistic monitoring system for measurement of the atmospheric electric field over the ocean - the sail campaign. In *Oceans 2022 - chennai* (p. 1-5). doi: 10.1109/OCEANSChennai45887.2022.9775273

Barbosa, S., & Karimova, Y. (2021). *SAIL Data Management Plan.* Zenodo. doi: 10 .5281/zenodo.4633444

Barbosa, S., Miranda, P., & Azevedo, E. (2017). Short-term variability of gamma radiation at the {ARM} eastern north atlantic facility (azores). *Journal of Environmental Radioactivity*, *172*, 218-231. doi: 10.1016/j.jenvrad.2017.03.027

Bossew, P., Cinelli, G., Hernández-Ceballos, M., Cernohlawek, N., Gruber, V., Dehandschutter, B., ... de Cort, M. (2017). Estimating the terrestrial gamma dose rate by decomposition of the ambient dose equivalent rate. *Journal of Environmental Radioactivity*, *166*, 296–308. doi: 10.1016/j.jenvrad.2016.02.013

Bottardi, C., Albéri, M., Baldoncini, M., Chiarelli, E., Montuschi, M., Raptis, K. G. C., ... Mantovani, F. (2020). Rain rate and radon daughters' activity. *Atmospheric Environment*, 117728.

Burnett, J. L., Croudace, I. W., & Warwick, P. E. (2010). Short-lived variations in the background gamma-radiation dose. *Journal of Radiological Protection*, *30*(3), 525.

Chambers, S. D., Williams, A. G., Conen, F., Griffiths, A. D., Reimann, S., Steinbacher, M., ... others (2016). Towards a universal "baseline" characterisation of air masses for high-and low-altitude observing stations using Radon-222. *Aerosol and Air Quality Research*, *16*, 885–899.

Cleveland, W., Grosse, E., & Shyu, W. (1992). Local regression models. chapter 8 in statistical models in s (jm chambers and tj hastie eds.), 608 p. *Wadsworth & Brooks/Cole, Pacific Grove, CA*.

Cortes, G., Sempau, J., & Ortega, X. (2001). Automated measurement of radon daughters bi-214 and pb-214 in rainwater. *Nukleonika*, *46*(4), 161–164.

Datar, G., Vichare, G., Raghav, A., Bhaskar, A., Sinha, A. K., & Nair, K. U. (2020). Response of Gamma-Ray Spectrum During Ockhi Cyclone. *Frontiers in Earth Science*, *8*, 15. doi: 10.3389/feart.2020.00015

Fisch, A., Eckley, I. A., & Fearnhead, P. (2018). A linear time method for the detection of point and collective anomalies. *arXiv preprint arXiv:1806.01947*.

Fujinami, N. (1996). Observational study of the scavenging of radon daughters by precipitation from the atmosphere . *Environment International*, *22, Supplement 1*, 181–185. (The Natural Radiation Environment {VI}) doi: 10.1016/ S0160-4120(96)00106-7

Greenfield, M. B., Domondon, A. T., Tsuchiya, S., Kubo, K., Ikeda, Y., & Tomiyama, M. (2003). Near-ground detection of atmospheric gamma rays associated with lightning. *Journal of Applied Physics*, *93*(3), 1839–1844. doi: 10.1063/1.1536731

Inomata, Y., Chiba, M., Igarashi, Y., Aoyama, M., & Hirose, K. (2007). Seasonal and spatial variations of enhanced gamma ray dose rates derived from 222Rn progeny during precipitation in Japan . *Atmospheric Environment*, *41*(37), 8043–8057. doi: 10.1016/j.atmosenv.2007.06.046

Ioannidou, A., Manolopoulou, M., & Papastefanou, C. (2005). Temporal changes of 7be and 210pb concentrations in surface air at temperate latitudes (40 n). *Applied Radiation and Isotopes*, *63*(2), 277–284.

Ioannidou, A., & Papastefanou, C. (2006). Precipitation scavenging of 7be and 137cs radionuclides in air. *Journal of Environmental Radioactivity*, *85*(1), 121–136.

Kaste, J. M., Norton, S. A., & Hess, C. T. (2002, 01). Environmental Chemistry of Beryllium-7. *Reviews in Mineralogy and Geochemistry*, *50*(1), 271-289. Retrieved from https://doi.org/10.2138/rmg.2002.50.6 doi: 10.2138/rmg .2002.50.6

Kusmierczyk-Michulec, J., Gheddou, A., & Nikkinen, M.   (2015).   Influence of precipitation on 7be concentrations in air as measured by ctbto global monitoring system. *Journal of Environmental Radioactivity*, *144*, 140–151.

Livesay, R., Blessinger, C., Guzzardo, T., & Hausladen, P. (2014). Rain-induced increase in background radiation detected by Radiation Portal Monitors. *Journal of Environmental Radioactivity*, *137*(Supplement C), 137–141.   doi: 10.1016/j .jenvrad.2014.07.010

Melintescu, A., Chambers, S., Crawford, J., Williams, A., Zorila, B., & Galeriu, D. (2018). Radon-222 related influence on ambient gamma dose. *Journal of Environmental Radioactivity*, *189*, 67–78. doi: 10.1016/j.jenvrad.2018.03.012

Mercier, J.-F., Tracy, B., d'Amours, R., Chagnon, F., Hoffman, I., Korpach, E., . . . Ungar, R. (2009). Increased environmental gamma-ray dose rate during precipitation: a strong correlation with contributing air mass . *Journal of Environmental Radioactivity*, *100*(7), 527–533. doi: 10.1016/j.jenvrad.2009.03.002

Paatero, J.   (2000, 02).   Wet deposition of radon-222 progeny in northern finland measured with an automatic precipitation gamma analyser. *Radiation Protection Dosimetry*, *87*(4), 273-280. doi: 10.1093/oxfordjournals.rpd.a033008

Paatero, J., & Hatakka, J. (1999). Wet deposition efficiency of short-lived radon-222 progeny in central Finland. *Boreal Env. Res.*, *4*, 285–293.

R Core Team.   (2022).   R: A language and environment for statistical computing [Computer software manual]. Vienna, Austria. Retrieved from `https://www.R -project.org/`

Takeuchi, N., & Katase, A. (1982). Rainout-Washout Model for Variation of Environmental Gamma-Ray Intensity by Precipitation. *Journal of Nuclear Science and Technology*, *19*(5), 393–409. doi: 10.1080/18811248.1982.9734160

Wessel, P., Luis, J., Uieda, L., Scharroo, R., Wobbe, F., Smith, W. H., & Tian, D. (2019).   The generic mapping tools version 6.   *Geochemistry, Geophysics, Geosystems*, *20*(11), 5556–5564.

Wessel, P., & Smith, W. H.   (1996).   A global, self-consistent, hierarchical, high-resolution shoreline database. *Journal of Geophysical Research: Solid Earth*, *101*(B4), 8741–8743.

Wilkening, M. H., & Clements, W. E.   (1975).   Radon 222 from the ocean surface. *Journal of Geophysical Research*, *80*(27), 3828–3830.

Yakovleva, V. S., Nagorsky, P. M., Cherepnev, M. S., Kondratyeva, A. G., & Ryabkina, K. S.   (2016).   Effect of precipitation on the background levels of the atmospheric beta- and gamma-radiation . *Applied Radiation and Isotopes*, *118*, 190–195. doi: 10.1016/j.apradiso.2016.09.017

Zafrir, H., Haquin, G., Malik, U., Barbosa, S., Piatibratova, O., & Steinitz, G. (2011).   Gamma versus alpha sensors for Rn-222 long-term monitoring in geological environments. *Radiation Measurements*, *46*(6-7), 611–620.   doi: 10.1016/j.radmeas.2011.04.027

Zelinskiy, A., Yakovlev, G. A., & Fil'Trov, D. (2021). Relation of gamma dose rate with the intensity of rain showers. *Bulletin KRASEC. Physical and Mathematical Siences*, *36*(3), 189–199.